

# Strong evaporative cooling of a trapped cesium gas

D. Guéry-Odelin, J. Söding, P. Desbiolles, and J. Dalibard

Laboratoire Kastler Brossel,<sup>†</sup> 24 rue Lhomond, 75005 Paris, France

dgo@physique.ens.fr

**Abstract:** Using forced radio-frequency evaporation, we have cooled cesium atoms prepared in the sublevel  $F = -m_F = 3$  and confined in a magnetic trap. At the end of the evaporation ramp, the sample contains  $\sim 7000$  atoms at 80 nK, corresponding to a phase space density  $3 \times 10^{-2}$ . A molecular dynamics approach, including the effect of gravity, gives a good account for the experimental data, assuming a scattering length larger than 300 Å.

©1998 Optical Society of America

**OCIS codes:** (020.0020) Atomic and molecular physics; (020.7010) Trapping; (020.2070) Effects of collisions; PACS 34.50.Pi, 03.75.Fi, 05.30.Jp, 32.80.Pj

<sup>†</sup> *Unité de recherche de l'ENS et de l'Université Pierre et Marie Curie, associée au CNRS.*

---

## References

1. M. H. Anderson, J. R. Ensher, M. R. Matthews, C. E. Wieman, and E. A. Cornell, *Science* **269**, 1989 (1995).
2. C. C. Bradley, C. A. Sackett, and R. G. Hulet, *Phys. Rev. Lett.* **78**, 985 (1997).
3. C. C. Bradley, C. A. Sackett, J. J. Tollet, and R. G. Hulet, *Phys. Rev. Lett.* **75**, 1687 (1995).
4. K. B. Davis, M.-O. Mewes, M. R. Andrews, N. J. van Druten, D. S. Durfee, D. M. Kurn, and W. Ketterle, *Phys. Rev. Lett.* **75**, 3969 (1995).
5. M. R. Andrews, C. G. Townsend, H.-J. Miesner, D. S. Durfee, D. M. Kurn, and W. Ketterle, *Science* **275**, 737 (1997).
6. E. A. Burt, R. W. Ghrist, C. J. Myatt, M. J. Holland, E. A. Cornell, and C. E. Wieman, *Phys. Rev. Lett.* **79**, 337 (1997).
7. J. Söding, D. Guéry-Odelin, P. Desbiolles, G. Ferrari, and J. Dalibard, accepted for publication in *Phys. Rev. Lett.*
8. A. Steane, P. Szriftgiser, P. Desbiolles, and J. Dalibard, *Phys. Rev. Lett.* **74**, 4972 (1995).
9. H. F. Hess, *Bull. Am. Phys. Soc.* [2] **30**, 854 (1985).
10. O. J. Luiten, M. W. Reynolds, and J. T. M. Walraven, *Phys. Rev. A* **53**, 381 (1996).
11. E. L. Surkov, J. T. M. Walraven, and G. V. Shlyapnikov, *Phys. Rev. A* **53**, 3403 (1996).
12. W. Ketterle and N.J. van Druten, *Adv. At. Mol. Opt. Phys.* **37**, 181 (1996).
13. H. Wu and C. Foot, *J. Phys. B*, **29**, L321-L328 (1996).
14. L. D. Landau and E. M. Lifshitz, *Quantum Mechanics* (Pergamon Press, Oxford, 1977), Sect. 143.
15. C. J. Joachain, *Quantum collision theory*, (North-Holland, Amsterdam, 1983) pp. 78-105
16. M. Arndt, M. Ben Dahan, D. Guéry-Odelin, M. W. Reynolds, and J. Dalibard, *Phys. Rev. Lett.* **79**, 625 (1997).
17. A. Fioretti, D. Comparat, A. Crubellier, O. Dulieu, F. Masnou-Seeuws, and P. Pillet, preprint (November 1997).
18. A. Kastberg, W. D. Phillips, S. L. Rolston, and R. J. C. Spreeuw, *Phys. Rev. Lett.* **74**, 1542 (1995).
19. D. Boiron, A. Michaud, P. Lemonde, Y. Castin, C. Salomon, S. Weyers, K. Szymaniec, L. Cagnet, and A. Clairon, *Phys. Rev. A* **53**, R3734 (1996).

## Introduction

The recent observation of Bose–Einstein condensation of atomic gases of rubidium [1], lithium [2, 3], and sodium [4] has attracted a lot of attention. These systems allow for quantitative tests of the theory of a dilute Bose gas. They also constitute a new source for atom optics and interferometry experiments, with coherence properties analogous to those of laser light [5, 6].

For the case of the heaviest stable alkali atom, *i.e.* cesium, which is at the basis of primary time and frequency standards, efforts to prepare a Bose–Einstein condensate have so far all foundered. We have recently measured the inelastic collision rate in an ultracold Cs sample prepared in its doubly polarized state ( $F = m_F = 4$ ) [7]. We observed a giant dipole relaxation that limited the maximal phase space density achievable by evaporative cooling to  $\sim 10^{-5}$ . In the present paper, we therefore focus on the study of the evaporative cooling of an atomic sample of Cs atoms in the lower hyperfine sublevel  $F = -m_F = 3$ . The atoms are confined around the magnetic field minimum of a Ioffe–Pritchard type trap. We obtain a cloud with an ultra-low temperature (80 nK), with a phase space density  $3 \times 10^{-2}$ , two orders of magnitude below the condensation threshold. Although we could not observe Bose–Einstein condensation, this constitutes a significant achievement due to the importance of cesium for metrology.

## Experimental setup

The apparatus is based on a double magneto-optical trap (MOT) system that has been described previously [8]. Atoms are collected in a MOT located in the upper cell ( $10^{-8}$  mBar of residual Cs vapor). This load, typically  $10^8$  atoms, is cooled by a short molasses phase (15 ms) and then falls down to the lower cell with a much better vacuum (residual pressure  $< 10^{-10}$  mBar). A large fraction of the atoms (70%) is recaptured in the lower MOT and cooled down to 6  $\mu$ K using again a short molasses phase.

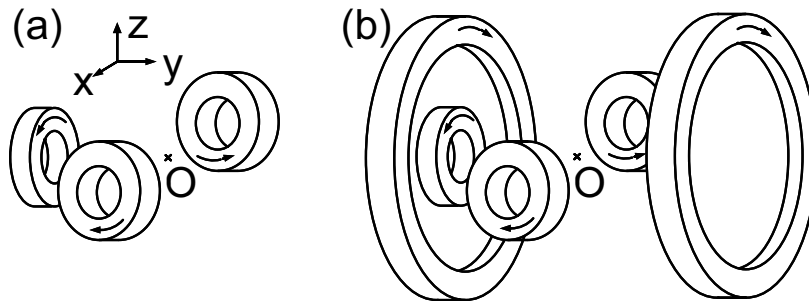


Figure 1. (a) Three-coil configuration for the magnetic trap. The two opposite coils are also used for the MOT. (b) Two extra Helmholtz coils are used to compress the atomic cloud in the  $xz$  plane.

The atoms are then optically pumped into the state  $F = -m_F = 3$  by applying a 500  $\mu$ s pulse of circularly polarized light, aligned with a magnetic field of  $2 \times 10^{-4}$  T, and resonant with the transition  $6S_{1/2}, F = 3 \leftrightarrow 6P_{3/2}, F' = 3$ . An additional beam resonant with the transition  $6S_{1/2}, F = 4 \leftrightarrow 6P_{3/2}, F' = 4$  depumps the atoms from the  $F = 4$  sublevel. The pumping efficiency is larger than 90%. We then switch on the magnetic trap, which is generated by a 50 A current running in three identical circular coils whose axes point towards  $+x$ ,  $-x$ , and  $+y$  respectively, where  $z$  denotes the vertical axis (fig. 1a). Each coil has 80 turns with an average diameter 34 mm, and it is located at 40 mm from the center  $O$  of the MOT, which coincides with the center of the magnetic trap. The resulting field configuration is equivalent to a Ioffe–Pritchard

type trap, with a non-zero local minimum of  $|\mathbf{B}(\mathbf{r})|$  in  $\mathbf{r} = \mathbf{0}$ . The leading terms in the field variations around  $O$  are  $(b'x, B_0 + b''y^2/2, -b'z)$ , with  $b' = 1.1 \text{ T/m}$ ,  $b'' = 60 \text{ T/m}^2$ , and  $B_0 = 1.1 \times 10^{-2} \text{ T}$ .

The trapped cloud is adiabatically compressed in 20 seconds by reducing the bias field  $B_0$  down to  $\sim 1.2 \times 10^{-4} \text{ T}$ , using a pair of Helmholtz coils centered on the magnetic trap (fig. 1b). After this compression, oscillation frequencies around the center of the trap are  $\nu_x = \nu_z = (3\mu b'^2/4mB_0)^{1/2}/2\pi = 87 \text{ Hz}$  and  $\nu_y = (3\mu b''/4m)^{1/2}/2\pi = 7 \text{ Hz}$  where  $\mu$  is the Bohr magneton, and  $m$  the atomic mass. At this stage, the cigar-shaped atomic cloud contains about  $5 \times 10^7$  atoms, at a temperature of  $120 \mu\text{K}$  and a peak density  $7 \times 10^{10} \text{ cm}^{-3}$ . The lifetime of the cloud due to the collisions with the residual background gas is 200 s.

We then evaporatively cool the atomic sample using forced evaporation. This technique relies on the thermalization of the sample *via* elastic collisions, while the particles in the high energy tail of the phase space distribution are being removed [9, 10, 12]. A radiofrequency wave (magnetic field amplitude  $3 \times 10^{-6} \text{ T}$ ) induces adiabatic transitions from the trapped Zeeman substate to an untrapped substate ( $m = -3 \rightarrow m = 3$ ). This energy selective transfer takes place on a surface  $\mu|\mathbf{B}(\mathbf{r})| = 4h\nu$  around the trap center. The RF frequency  $\nu$  is ramped down linearly in 30 seconds, from 4000 kHz to an adjustable final frequency. From the final frequency  $\nu_0$  which expels all atoms (427 ( $\pm 3$ ) kHz), we determine precisely the bias field  $B_0 = 1.17 (\pm 0.01) \times 10^{-4} \text{ T}$ , taking into account the effect of gravity (see below).

### Temperature and density measurements

The cooled cloud is probed by absorption imaging. The current in the magnetic trap coils is switched off in less than  $500 \mu\text{s}$ . The atoms are pumped into the  $F = 4$  sublevel using a  $200 \mu\text{s}$  light pulse resonant with the  $6S_{1/2}, F = 3 \leftrightarrow 6P_{3/2}, F' = 3$  transition. The cloud is then briefly ( $80 \mu\text{s}$ ) illuminated by a circularly polarized imaging laser beam, propagating along the  $x$  axis and resonant with the  $6S_{1/2}, F = 4 \leftrightarrow 6P_{3/2}, F' = 5$  transition. The shadow produced by the cloud in this beam is imaged with a magnification 2.47 onto a CCD array (optical resolution  $7 \mu\text{m}$ ). The image is then digitally processed to extract the column density of the cloud  $\int n(x, y, z) dx$ , where  $n(\mathbf{r})$  is the spatial density. This quantity is well fitted by a 2D Gaussian function as expected for a thermal distribution in a harmonic trap. Assuming rotational symmetry around the  $y$ -axis, we then deduce all relevant quantities such as the number of atoms  $N$  and the temperature  $T$ . We evaluate  $T$  using only the size of the cloud along the  $y$  axis, so that the optical resolution of our detection scheme is not a limit, even for the lowest measured temperature. For instance a *rms* size along  $y$  equal to  $51.5 \mu\text{m}$  corresponds to a cloud at  $T = 80 \text{ nK}$ .

We have performed an independent measurement of the temperature based on a time-of-flight analysis. After the preparation of the cloud at the desired temperature, we abruptly switch off the magnetic trap, let the cloud expand ballistically for an adjustable time  $\tau$ , and take an image. The time of flight  $\tau$  is varied from 1 ms up to 13 ms, with 1 ms steps. A typical resulting set of pictures is shown in figure 2. We fit the evolution of the *rms* size along the  $z$  axis by  $(\Delta z_0^2 + \Delta v^2(t - t_0)^2)^{1/2}$ , with the three adjustable parameters  $\Delta z_0$ ,  $\Delta v$  and  $t_0$ . From  $\Delta v$  we deduce the temperature  $T = m\Delta v^2/k_B = 1.0 \mu\text{K}$ , to be compared with the value  $0.76 \mu\text{K}$ , deduced from the  $y$  size at  $\tau = 0$ . The analysis of several sets of similar data for initial conditions in the micro-Kelvin domain show that the results of these two methods agree with each other to within  $\pm 25\%$ .

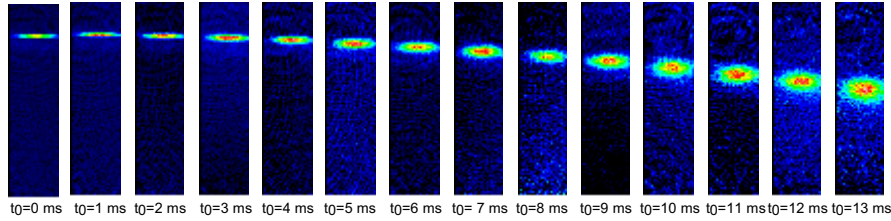


Figure 2. Time of flight analysis: the atoms are released from the magnetic trap at time  $\tau = 0$ . We deduce the temperature from the vertical expansion of the cloud.

### The role of gravity

To analyze quantitatively the dynamics and the results of the evaporation experiment, we have to take into account gravity which plays an important role due to the large mass of the Cs atoms. The potential along the  $z$  axis is now:

$$W(z) = \frac{3\mu}{4} \sqrt{B_0^2 + b'^2 z^2} + mgz$$

Consequently the potential minimum is displaced to

$$z_0 = - \left( \epsilon / (1 - \epsilon^2)^{1/2} \right) B_0 / b' \quad ,$$

where  $\epsilon = 4mg/(3b'\mu)$  is of the order of 0.3 for our setup. The harmonic approximation around the bottom of the potential remains valid since  $\epsilon^2 \ll 1$ . On the  $z$  axis, the RF induces spin flips at

$$\frac{\mu}{4} \sqrt{B_0^2 + b'^2 z^2} = h\nu$$

The critical value  $\nu_0$  which expells all atoms is obtained by taking  $z = z_0$  in the above formula, which leads to:

$$B_0 = \frac{4h\nu_0}{\mu} (1 - \epsilon^2)^{1/2}$$

to be compared with the result  $B_0 = 4h\nu_0/\mu$  when gravity can be neglected. As pointed out in [11, 12], gravity also changes the dynamics of RF-induced evaporation. For temperatures below 20  $\mu\text{K}$ , the gravitational energy varies in our setup by more than  $2k_B T$  over the evaporation surface. In this regime the atoms only escape from the trap near the bottom (1D evaporation), which limits severely the efficiency of evaporative cooling.

### Numerical simulation of the evaporation

In order to give a quantitative theoretical account for the evaporation, we have developed a numerical simulation of the motion of the atoms in the magnetic trap within the harmonic approximation. This approach consists in a molecular dynamics evolution of the atomic sample. It allows a precise description of the atomic dynamics in the present trap, where atoms above the evaporation threshold may still be confined for some trajectories, owing to the 1D character of the evaporation.

In order to conveniently deal with an atom number which varies by 4 orders of magnitude from the beginning to the end of the evaporation, we have used a duplication technique. We evolve a distribution of macro-atoms, whose number is maintained between 4000 and 8000, to be compared with the  $5 \times 10^7$  real atoms initially present. Each macro-atom represents  $p$  real atoms, with  $p = 2^{13} = 8192$  at the beginning of the simulation shown below. Each macro-atom has the same mass and the same magnetic moment as a Cs atom. The collisional cross-section between two macro-atoms is

$p$  times larger than the collisional cross-section for two real atoms with the same velocity. Each time the number of macro-atoms becomes lower than 4000, either because of evaporation or because of losses simulating collisions with the residual gas, every macro-atom is replaced by two new macro-atoms, each of which represents only  $p/2$  atoms. If the parent macro-atom is in  $(x, y, z)$  with velocity  $(v_x, v_y, v_z)$ , one of two new macro-atoms is placed at the same point with the same velocity, and the other one is placed in  $(-x, -y, z)$  with the velocity  $(-v_x, -v_y, v_z)$ . This duplication, which exploits the symmetry of the trap, guarantees that these two new macro-atoms will not undergo a collision with each other immediately after the duplication process. The duplication process stops when  $p$  is equal to 1.

The collisions between the macro-atoms are taken into account using a boxing technique [13]. After each evolution time step  $\delta t$ , the position of each particle is discretized with a step  $\delta r$ , so that each particle is assigned to a cubic box of volume  $\delta r^3$ . The number of boxes is  $3.5 \times 10^5$ ; the size  $\delta r$  is adjusted as the cloud cools down, so that the probability for having two particles in the same box is much smaller than 1. When two macro-atoms are found in the same box, a collision may take place between them. The probability for this collision is  $p \sigma(k) v \delta t / \delta r^3$ , where  $k$  and  $v = 2\hbar k/m$  are the relative wave vector and velocity of the colliding particles, and  $\sigma(k)$  the collisional cross section between two real Cs atoms. The time step  $\delta t$  is chosen such that this probability is small compared to 1. The occurrence of a collision is then randomly decided. The collision is isotropic since only the  $l = 0$  partial wave contributes at these ultra-low temperatures. We put [14, 15, 16]

$$\sigma(k) = \frac{8\pi a^2}{1 + k^2 a^2} \quad , \quad (1)$$

where  $a$  is the scattering length. At very low relative velocity one recovers the well known limit  $\sigma = 8\pi a^2$ , while one obtains for higher velocities the unitary limit  $\sigma(k) = 8\pi/k^2$ , corresponding to the result for a zero-energy resonance [16].

## Results

We show in figures 3a and 3b the evolution of the number of trapped atoms and of their temperature in an evaporation sequence. The images used for these measurements are depicted in figure 4. We use an evaporation ramp in which the frequency is ramped linearly from 4000 kHz down to 435 kHz in 30 seconds. The cloud at the end of the evaporation ramp contains  $\sim 6500$  ( $\pm 1500$ ) atoms at  $80$  ( $\pm 20$ ) nK.

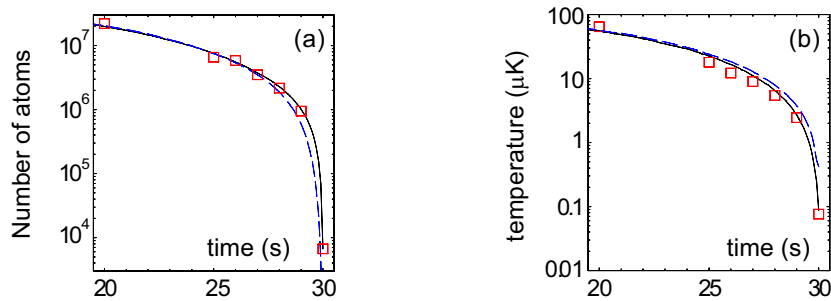


Figure 3. Evolution of (a) the number of atoms and (b) the temperature during the 10 last seconds of the evaporation ramp. Experimental data:  $\square$ , numerical simulation: continuous line ( $|a| = 1000 \text{ \AA}$ ), dashed line ( $|a| = 100 \text{ \AA}$ ).

We have also plotted in figs. 3a,b the predictions of the numerical simulation describing the motion and the evaporation of the atoms in the trap for  $|a| = 100 \text{ \AA}$  and

$|a| = 1000 \text{ \AA}$ . Both scattering lengths lead to the same results until the two last seconds of the ramp. Indeed for  $t \leq 28 \text{ s}$ , the temperature is large enough for the unitary approximation  $\sigma(k) \simeq 8\pi/k^2$  to be valid for both  $a$ 's. For  $t = 30 \text{ s}$ , the predictions of the simulation concerning the remaining number of atoms  $N$  and the final temperature  $T$  are summarized in table 1. The best agreement with the experimental data is obtained for  $|a| > 300 \text{ \AA}$ . Such a large value for the scattering length is in good agreement with recent measurements based on photoassociation experiments [17] (see also [16]).

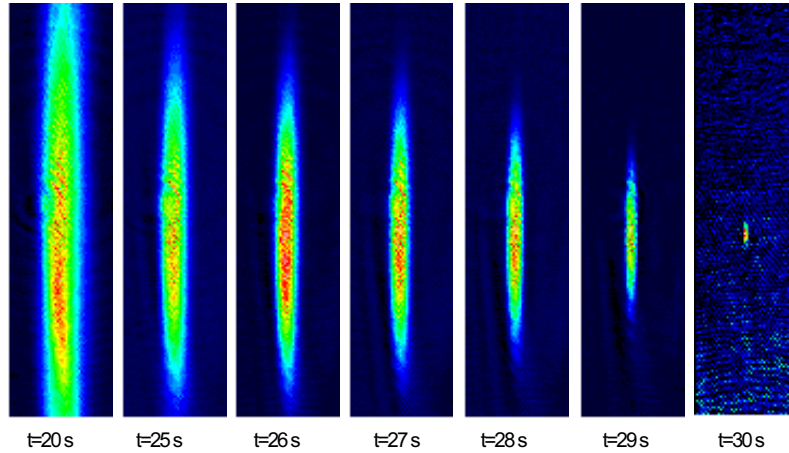


Figure 4. Series of pictures taken  $t$  seconds after the start of a 30 seconds linear evaporation ramp.

The corresponding phase space density is shown in figure 5. It starts from  $2 \times 10^{-7}$ , typical of a compressed magneto-optical trap, and it ends at  $3 \times 10^{-2}$ , a factor 100 below Bose-Einstein condensation. The set of data between 25 and 29 seconds exhibits a clear “runaway evaporation”: the product of the density times the *rms* velocity remains constant, although the number of atoms is divided by 7. For a velocity-independent collisional cross section, this would mean a constant collisional rate. In our case, where the cross section varies as  $1/T$  in this region (unitary limit of eq.1), the situation is even more favourable since the collisional rate increases by 4.

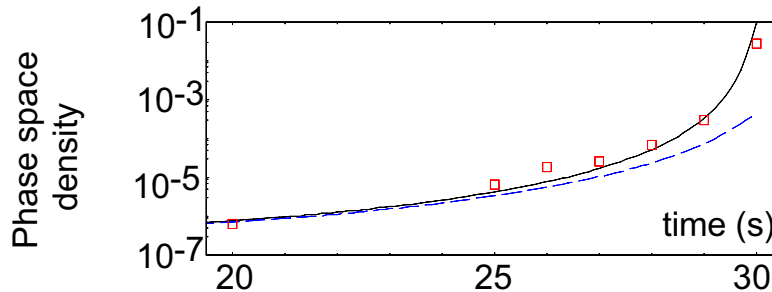


Figure 5. Evolution of the atomic phase space density during the 10 last seconds of the evaporation ramp. Experimental data:  $\square$ , numerical simulation: continuous line ( $|a| = 1000 \text{ \AA}$ ), dashed line ( $|a| = 100 \text{ \AA}$ ).

The last data point ( $t = 30 \text{ s}$ ) corresponds to a cloud whose expected transverse extension is  $4 \mu\text{m}$ , estimated from the measurement of the longitudinal dimension of the cloud ( $52 \mu\text{m}$ ) and from its expected ellipticity ( $\sim 13$ ). This is below the resolution of our optical system and indeed the measured size ( $\sim 7 \mu\text{m}$ ) is larger than this expected

value. To evaluate the spatial density and the phase space density, we have not corrected the transverse dimension by imposing a constant ellipticity, which leads therefore to a conservative value for the largest achieved phase space density.

Table 1. Predictions of the numerical simulation for the result of the evaporation, for various scattering lengths.

$a$ (Å)	50	100	200	300	500	1000	2000	experiment
$N$	0	200	1600	3600	5600	6600	7000	6500 ( $\pm$ 1500)
$T$ (nK)	–	420	230	190	120	90	90	80 ( $\pm$ 20)

## Conclusion

We have used forced RF evaporation to produce an ultra-cold cesium gas at 80 ( $\pm$ 20) nK. This temperature is 10 times lower than what has been achieved up to now for cesium with optical cooling in 3D [18, 19], and is well below the single photon recoil limit (200 nK). We could achieve the runaway regime at  $t \geq 25$  s in the data set of figs. 3 and 5. This indicates that, with an optimized evaporation ramp, BEC should be reachable with more than 5000 condensed atoms [10]. Our numerical simulations confirm this prediction: for instance a 90 seconds linear ramp starting with the same initial conditions should lead to condensation if  $|a| \geq 250$  Å. However we could not increase the phase space density above the present maximal value  $3 \times 10^{-2}$ . Indeed we have observed for these ultra-cold clouds density dependent losses, accompanied by a heating of the atoms when the RF shield is removed. These loss processes, which we attribute to inelastic collisions between trapped atoms, are currently under study.

We are grateful to G. Ferrari, M. Arndt, and M. Ben Dahan for their assistance and to C. Cohen-Tannoudji, C. Salomon, and the LKB group for discussions. J. S. acknowledges support by the Alexander von Humboldt-foundation. This work was partially supported by CNRS, Collège de France, DRET, DRED and EC (TMR network ERB FMRX-CT96-0002).